



Echinocystic acid provides a neuroprotective effect via the PI3K/AKT pathway in intracerebral haemorrhage mice

Beilei Chen^{1,2,3#}, Yuanyuan Zhao^{2,3#}, Wei Li^{2,3#}, Jing Hang^{1,2}, Mengmei Yin^{1,2}, Hailong Yu^{1,2,4}

¹Clinical Medical College of Yangzhou University, Yangzhou 225009, China; ²Department of Neurology, Northern Jiangsu People's Hospital, Yangzhou 225001, China; ³Dalian Medical University, Dalian 116044, China; ⁴Affiliated of Drum Tower Hospital, Medical school of Nanjing University, Nanjing 210008, China

Contributions: (I) Conception and design: B Chen, H Yu, Y Zhao, W Li; (II) Administrative support: None; (III) Provision of study materials or patients: Y Zhao; W Li, J Hang, M Yin; (IV) Collection and assembly of data: H Yu, Y Zhao, W Li; (V) Data analysis and interpretation: Y Zhao, W Li, J Hang, M Yin; (VI) Manuscript writing: All authors; (VII) Final approval of manuscript: All authors.

[#]These authors contributed equally to this work.

Correspondence to: Hailong Yu. Clinical Medical College of Yangzhou University, Yangzhou 225009, China. Email: hailongyu1982tg@163.com.

Background: Echinocystic acid (EA), a natural extract from plants of *Gleditsia sinensis* Lam, exhibits anti-inflammatory, antioxidant and analgesic activities in different diseases. In this study, we explored the pharmacological effects of EA on intracerebral haemorrhage (ICH) in a collagenase-induced ICH mouse model.

Methods: EA (50 mg/kg, i.p. q.d) was injected after the establishment of ICH, and we measured the amount of degraded neurons in brain tissue with Fluoro-Jade C staining and the haemorrhagic injury volume with Luxol fast blue staining on day 3 after ICH. We also assessed animal behaviour by rotarod test, claw force test and modified neurological severity score (mNSS) score. The expression of apoptosis-related proteins such as Bcl-2, Bax and cleaved caspase-3 was analysed by Western blot.

Results: EA reduced both the death of neurons and the volume of haemorrhagic injury after ICH. The haemorrhage infarct volume of the ICH+EA group was 9.84%±3.32% lower than that in the ICH group of mice ($P<0.01$). The mNSS score of the ICH+EA treated group was 4.75±0.55 lower than that in the ICH group ($P<0.01$). With the administration of EA after ICH, the expression of Bcl-2 was upregulated while the Bax level was downregulated. The cleaved caspase-3 level was also significantly decreased. We further investigated the neuroprotective mechanism of EA. Western blot results showed that the expression of P-AKT increased after EA treatment and decreased after LY294002, an inhibitor of the PI3K/AKT pathway, treatment.

Conclusions: EA may provide neuroprotection via activation of the PI3K/AKT pathway. Given the safety of EA has been proven, further studies are required to investigate whether EA is a potential agent for the treatment of ICH.

Keywords: Intracerebral haemorrhage (ICH); echinocystic acid (EA); anti-apoptotic; PI3K/AKT pathway

Submitted Sep 03, 2019. Accepted for publication Nov 06, 2019.

doi: 10.21037/atm.2019.12.35

View this article at: <http://dx.doi.org/10.21037/atm.2019.12.35>

Introduction

Intracerebral haemorrhage (ICH) is a serious and common neurological disorder that accounts for 15% of all stroke cases and has a 30–67% mortality and poor prognosis in

all patients (1,2). Although many studies on ICH have been performed, there is still no effective neuroprotective treatment available (3). The primary damage resulting from ICH is the compression effect of haematoma due to the rapid accumulation of blood, which causes approximately

half of all deaths due to ICH (1). The most likely toxic substances released from lysed red blood cells, such as haemoglobin and oxidative stress and inflammatory factors, contribute to the secondary damage to brain tissue (4-6). During the two stages of damage after ICH, different pathological processes lead to many types of cell death, including apoptosis and necrosis (7). Many studies have shown negative results in terms of reversing necrosis in nerve tissue, so alleviating or reducing the apoptosis of nerve cells is considered an important target in the treatment of ICH (8). However, many drugs that have shown anti-apoptotic effects in animal models of ICH have failed in clinical trials (9). Thus, we still need to find safe and effective agents for the treatment of ICH.

Echinocystic acid (EA) is a natural extract from the plants of *Gleditsia sinensis* Lam (10). The safety of EA has been widely proven, and EA has been reported in the use of food and traditional Chinese medicine in many Asian countries (11). Many studies have found that EA has several positive effects in terms of its anti-inflammatory and antioxidant characteristics in acute diseases (12,13). Interestingly, existing studies also appear to present contradictory conclusions. EA has been shown to provide anticancer abilities to induce apoptosis in tumour cells; however, in the nervous system, EA promotes the proliferation and growth of nerve protrusion in the hippocampal regions of elderly mice (14,15). Therefore, EA may have different pharmacological effects in different diseases, which may explain the contradictory results. Recent studies have shown that EA ameliorates hyperhomocysteinaemia-induced vascular endothelial cell injury by regulating NF- κ B (16). These results suggest that EA is beneficial in neurological diseases. However, whether EA has a neuroprotective effect on ICH remains unclear. Based on EA's anti-inflammatory and antioxidant characteristics, we assume that EA may provide a neuroprotective effect in ICH. In short, we used a cerebral haemorrhage mouse model to explore the neuroprotective effects of EA and to determine underlying mechanisms.

Methods

Materials

EA was purchased from Nanjing Spring & Autumn Biological Engineering Co. Ltd, with a purity greater than 98%. Rabbit beta-tubulin polyclonal antibody, rabbit beta-

actin polyclonal antibody, rabbit anti-Bcl-2 and rabbit anti-Bax were purchased from Bioworld Technology Inc. (St Louis Park, MN, USA); Rabbit anti-cleaved caspase-3, rabbit anti-AKT and rabbit anti-p-AKT were purchased from Cell Signaling Technology, Inc. (Danvers, MA, USA). Collagenase IV was purchased from Sigma-Aldrich Company (St Louis, MO, USA). LY294002 was purchased from Selleck Chemicals (Houston, USA). Fluoro-Jade C (FJC) was purchased from Affiliate of Merck KGaA, Darmstadt, Germany. Solvent Blue 38 was purchased from Sigma-Aldrich. The ECL chemiluminescence system was purchased from Thermo Company (Rockford, IL, USA).

Animals

All adult male ICR mice (8–10 weeks, 25–30 g) were purchased from the Comparative Medical Centre of Yangzhou University. The animals were housed under conditions of 22 ± 2 °C and 60% humidity with a 12 h light/dark cycle. The animals were fed plenty of food and water. All experimental procedures were approved by the Animal Ethics Committee of Yangzhou University (license number: YIACUC-14-0014).

Experimental groups

The animals were randomly assigned to five groups of eight animals each: the (I) vehicle-treated group (sham); (II) EA-treated group (EA group); (III) vehicle-treated ICH group (ICH group); (IV) EA-treated ICH group (ICH + EA group); and (V) LY294002-treated ICH + EA group (ICH + EA + LY294002). The neuroprotective effects of EA occurred in a dose-dependent manner. We found that EA had the best brain protection at 50 mg/kg intraperitoneal injection (17). EA was intraperitoneally injected (i.p.) at 50 mg/kg of body weight for 3 days after the mouse model was established in the ICH+EA and EA groups. The animals were injected immediately after anaesthesia once a day for 3 consecutive days. The animals were intraperitoneally injected with equal volumes of vehicle in the sham and ICH groups. The PI3K inhibitor LY294002 [i.p. 5 μ L of 10 mM LY-294002 dissolved in 3% dimethyl sulfoxide (DMSO)] was injected 15 min before cerebral haemorrhage once a day for 3 consecutive days, and EA was injected at the above dosage in the ICH + EA + LY294002 group. In the sham group, mice were anaesthetized in the same manner, and their scalps were cut open and sutured.

The ICH model

Intraperitoneal chloralhydrate was used to anaesthetize the mice, and then the animals were fixed in a stereoscopic locator. The coordinates used were located in the striatum of the mice. A small incision was made to expose the skull. A high-speed drill was used to make a burr hole. A total of 0.04 units of CollagenaseIV dissolved in 0.6 μ L of phosphate buffered saline (pH 7.4, PBS) was microinjected at a speed of 0.2 μ L/min into the left striatum (3.0 mm) under stereotaxic guidance. The needle was held in place for another 5 min after the infusion to prevent leakage. After the syringe was removed, bone wax was used to seal the bone pores. Then, the scalp was sutured. During the operation, the room temperature was kept at 25 °C. The mice were placed on an electric blanket to maintain their rectal temperature at 37 °C until palinesthesia (18).

Behavioural evaluation of the mice

Rotarod test

Mice move in the opposite direction of a rotating rod. During strenuous exercise, lactic acid builds up and muscles quickly tire out. The effects of CNS injury on motor coordination function and fatigue can be evaluated by measuring the duration that animals spend walking on a roller. Three days before the mouse model was established, the mice were trained, and the rod rotation fatigue instrument was set at 10, 20 and 30 rotations per min. Each time the mice were trained for 5 min, the interval was at least 30 min. Training occurred twice a day, with at least 2 h between each training session. For the following 2 days, the rod was set to rotate at 20, 30, and 40 revolutions per minute. The resting time was the same as before. On the third day after the mouse model was established, the time the mice spent on the rotating rod was assessed at a speed of 40 revolutions per minute for a total of three times. The longest duration of the three tests was used. All sham group and EA group mice did not fall off the rod for 2 min.

Modified neurological severity score (mNSS) for the mouse behavioural tests

The mNSS is used to evaluate the neurological deficits of mice in terms of motor, reflex, sensory, and balance tests. A higher score indicates more severe injury. The mice were scored on the third day after the mouse model was established.

Claw strength tests

Mice are held by the tail until they grasp a dynamometer. When the mice grasp the metal bar at the front of the dynamometer, the appropriate force pulls the mice horizontally and backward. The test was performed 5 times, with 5 s in between each test, and the maximum value was used.

Preparation of frozen sections of tissues

The animals were anaesthetized by injecting intraperitoneal chloralhydrate and perfused transcranially with 50 mL of phosphate buffered saline, followed by 50 mL of 4% paraformaldehyde. The brains were removed via decapitation and were submerged overnight in 4% paraformaldehyde. The brains continued to soak in 15%, 25% and 30% successive intervals of sucrose solution for gradient dehydration. After the brains sank to the bottom of the tube, they were frozen overnight at -80 °C in the refrigerator. Frozen coronal slices (20 μ m) were obtained on a frozen slicer (CM3050S, Leica Microsystems).

FJC staining

FJC staining was performed using FJC dye according to the manufacturer's instructions. The sections were visualized using a fluorescence microscope (FV1200; Olympus Corporation). Degenerated neurons appeared with green fluorescence. The extent of neuronal damage was evaluated with ImageJ software (ImageJ 1.5, NIH, USA) as the average number of FJC-positive neurons in eight sections per brain. The data are presented as the average number of FJC-positive neurons in 40 \times high-magnification fields.

Luxol fast blue (LFB) myelin staining

LFB staining was used to assess the haemorrhagic injury volume 3 days after ICH. Slices were dried at 37 °C for 10 min, washed in ddH₂O for 2 min, and submersed in 95% ethanol for 1 min. The slices were incubated with 0.1% LFB at 60 °C for 2 h and were allowed to dry for half an hour. The slices were washed with ddH₂O and were differentiated with 0.05% lithium carbonate solution and 70% ethyl alcohol for 10 s each. The tissues were gradually dehydrated with an ethanol gradient (70%, 85%, 95% and 100%) and fixed with xylene. Damaged brain tissue appeared as white, while healthy tissue appeared as blue. The LFB-stained sections were quantitatively analysed. The ratio of the white damaged area to the contralateral blue area was calculated with ImageJ software.

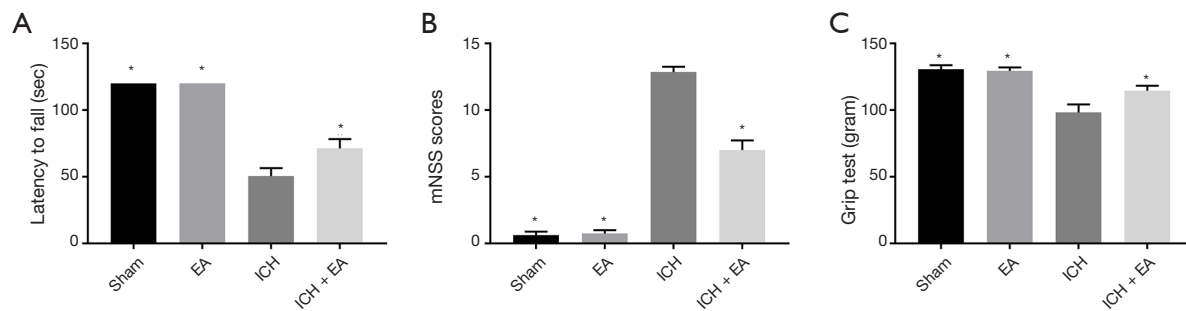


Figure 1 Echinocystic acid (EA) treatment reduced neurological deficits after intracerebral haemorrhage (ICH). Mice were administered (i.p.) EA or an equal volume of vehicle continuously for three days after the mouse model of cerebral haemorrhage was established. Neurological deficits were examined after 3 days of ICH. EA treatment significantly decreased neurological deficits. (A) Latency to fall time in the rod rotation experiment; (B) modified neurological severity score (mNSS) in each group of mice after 3 days of ICH; (C) comparison of the grasping force in each group. Before the experiment, there were no statistically significant differences in claw force or body weight in each group. The bar graphs represent the mean \pm S.E.M. of 8 mice in each group, *, $P < 0.05$ compared with the ICH group.

Western blot analysis

Three days after modelling, the animals were sacrificed. The brains were quickly removed, and pericerebral haemorrhage brain tissues were collected. Proteins were homogenized in RIPA lysis buffer (Millipore, Billerica, MA, USA) containing protease inhibitors. The supernatant was assayed using a BCA Protein Assay Kit (Thermo-Fisher Scientific, MA, USA). The protein concentration was adjusted to the same concentration with protein buffer. Protein electrophoresis was carried out with 12.5% sodium dodecyl sulfate-polyacrylamide gel electrophoresis (SDS-PAGE), and then the samples were electrotransferred to 0.2 μ m nitrocellulose membranes. Blots were blocked with phosphate buffered saline/0.1% Tween 20 (PBST) containing 5% non-fat dry milk for 2 h. After washing with PBST, the blots were incubated with primary antibody at 4 $^{\circ}$ C overnights. After washing with PBST, the blots were incubated with HRP-conjugated secondary antibody in blocking solution for 2 h and were then developed with the ECL chemiluminescence system (Thermo Company, West Chester, Pennsylvania, USA). At the same time, immunoreactive bands were captured on autoradiographic films (Kodak Company, Rochester, New York, USA). The films were then digitalized with a camera, and densitometric analysis of the bands was performed using Alpha Ease Image Analysis Software.

Statistical analysis

All statistical and graphical analyses were performed using ImageJ and GraphPad Prism 7.0, respectively. All data

were analysed using t-test or one-way analysis of variance (ANOVA). All data are presented as the mean with S.E.M. $P < 0.05$ was considered statistically significant.

Results

EA treatment improved ICH mouse symptoms of neurological impairment

There is evidence that EA has anti-inflammatory and antioxidation effects as well as analgesic activities. To further study the effect of EA on cerebral haemorrhage, we conducted continuous intraperitoneal injections of EA for three days after the mouse model of cerebral haemorrhage was established and then tested the grasping power of the mice, duration to fatigue in the rod rotation experiment, and mNSS. No significant difference was observed between the sham group and the drug therapy groups. The effects of grasping power after EA treatment in ICH mice are shown in panel C of Figure 1. The grasping force in the ICH group (98.35 ± 5.99 g, $n=8$) was significantly lower than that in the ICH + EA group (114.50 ± 3.84 g, $n=8$, $P < 0.05$). Furthermore, the rod-rotation persistence time in the EA + ICH group (71.25 ± 7.09 s, $n=8$) was also significantly different from that in the ICH group (50.50 ± 6.11 s, $n=8$, $P < 0.05$), as shown in Figure 1A. Regarding the mNSS, the ICH + EA group (7.87 ± 0.35 , $n=8$) was significantly different from the ICH group (12.63 ± 0.42 , $n=8$) ($P < 0.05$, Figure 1B). There were no statistically significant differences in body weight, claw force or rod-rotation persistence time between the groups before the model was established and the drug was administered.

EA had a positive effect on reducing both the injured area from cerebral haemorrhage and neuron apoptosis

LFB staining can reveal damage to the myelin sheaths of nerves, which in turn can reveal the area of damage during cerebral haemorrhage. The white part area represents the damaged part, and the blue area represents the normal part of the tissue. We stained the prepared frozen sections of each group and measured the ratio of the surviving blue parts of tissue on the damaged side to the contralateral brain area. The results showed that EA markedly reduced the haemorrhage volume. EA-treated mice in the ICH+EA group had a large total surviving volume ($79.79\% \pm 2.79\%$), which was significantly higher than that in the ICH group of mice ($69.95\% \pm 1.78\%$, $P < 0.01$, panel B and D of *Figure 2*, panel A and C of *Figure 3*). FJC staining can verify neuronal degeneration and apoptosis. As shown in *Figure 2C,E*, compared to the sham group (43.00 ± 2.91), the ICH group demonstrated a significant increase in the number of FJC-positive neurons in the ipsilateral cerebral haemorrhage cortex (176.10 ± 4.80 , $P < 0.05$, *Figure 2E*). However, the number of FJC-positive neurons was significantly decreased after EA treatment (122.40 ± 5.35 , $P < 0.05$, *Figure 2E*).

EA therapy regulated the expression of apoptotic proteins after ICH

Because EA reduced apoptosis in neurons after cerebral haemorrhage, we hypothesized that this phenomenon might be related to apoptosis. We examined the expression levels of Bcl-2 and Bax, two important markers of apoptosis, 3 days of cerebral haemorrhage was established. We found that EA treatment increased the level of Bcl-2 expression ($P < 0.05$, *Figure 3A,C*) and decreased the level of Bax expression compared with the ICH group ($P < 0.05$, *Figure 3A,D*). We then calculated the Bcl-2/Bax ratio, which is an important marker of neuronal apoptosis. Our results showed that EA treatment markedly increased the Bcl-2/Bax ratio after cerebral haemorrhage ($P < 0.05$, *Figure 3E*). This indicated that EA could inhibit apoptosis by regulating the Bcl-2/Bax ratio. At the same time, as a classic marker of apoptosis, the level of cleaved caspase-3 in the ICH group (2.52 ± 0.06 , $n=3$) was significantly higher than that in the sham group (1.00 ± 0.11 , $n=3$), indicating that apoptosis is involved in cerebral haemorrhage injury. The level of cleaved caspase-3 was also significantly decreased with the administration of EA (1.54 ± 0.10 , $n=3$) compared with the

ICH group ($P < 0.05$, *Figure 3B,F*).

EA treatment changed the expression level of phosphorylated AKT (p-AKT)/AKT in brain tissue after cerebral haemorrhage injury

To investigate the mechanism of the inhibition of apoptosis by EA, we assessed brain tissues after three days of intraperitoneally injecting drugs and after ICH injury and EA treatment and measured the levels of p-AKT and AKT (AKT). EA treatment increased the level of p-AKT compared with the ICH group (panel A of *Figure 4*). The ratio of p-AKT to AKT was significantly higher in the ICH group (1.76 ± 0.15 , $n=3$) than in the sham group (1.00 ± 0.08 , $n=3$). With cerebral haemorrhage, EA significantly increased the ratio of p-AKT/AKT compared with the ICH group (2.49 ± 0.12 , $n=3$, $P < 0.05$, *Figure 4A,D*). This finding indicates that the PI3K/AKT pathway is involved in the anti-apoptosis activity of EA.

The PI3K inhibitor LY294002 removed the protective effect of EA on cerebral haemorrhage

To further confirm that the PI3K/AKT pathway indeed plays an important role in the cerebral protective effect of EA, we treated mice with the PI3K inhibitor LY294002 (i.p. 5 μ L of 10 mM LY294002 dissolved in 3% DMSO) 15 min before cerebral haemorrhage once a day for 3 consecutive days. Then, we intraperitoneally injected the mice with EA for three days in the same manner as described earlier. Next, Western blot analysis of brain tissue proteins was performed. The results showed that the PI3K inhibitor LY294002 inhibited the growth of p-AKT (*Figure 4B*). FJC staining also confirmed that the injury of nerve cells after the use of the LY294002 inhibitor (148.90 ± 4.16 , $n=6$) was significantly increased compared with the EA treatment group after cerebral haemorrhage (122.40 ± 5.35 , $n=6$, *Figure 4C,E*). These results showed that the PI3K inhibitor LY294002 removed the protective effect of EA on cerebral haemorrhage. This finding further demonstrates that the PI3K/AKT pathway mediates the neuroprotective effect of EA after cerebral haemorrhage.

Discussion

There were two novel findings in our study. First, the results demonstrated that EA provided neuroprotective effects in ICH via its anti-apoptotic characteristics (*Figures 1–3*). Second, we specifically investigated the involvement of the PI3K/AKT signalling pathway in the anti-apoptotic effect

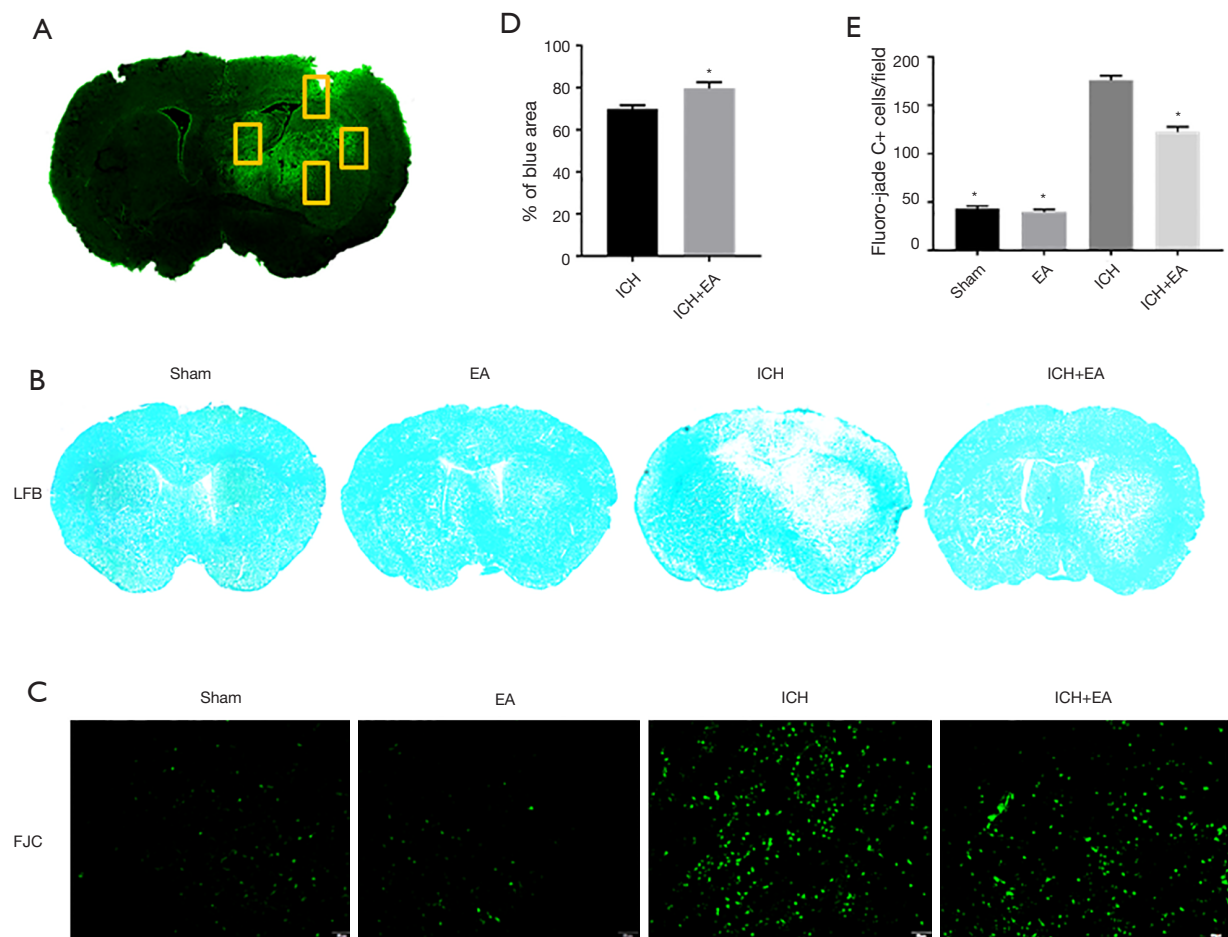


Figure 2 Echinocystic acid (EA) treatment reduced the injured area of cerebral haemorrhage and neuron apoptosis. Green fluorescence in FJC staining indicates neuronal injury or neuronal apoptosis. In Luxol fast blue (LFB) staining, white indicates the damaged part, and blue indicates the normal part of the tissue. The pictures show that EA markedly reduced haemorrhagic injury volume and neuron apoptosis. (A) FJC staining at 4× high-magnification fields. (B,D) LFB staining reveals the area of damage during cerebral haemorrhage. Analysis the ratio of the surviving blue parts on the damaged side to the contralateral brain area in the intracerebral haemorrhage (ICH) or ICH + EA group. EA reduced the volume after ICH injury. Bars represent the mean \pm S.E.M. of 6 brains. *, $P < 0.05$ versus vehicle-treated ICH group. (C) FJC staining at 40× high-magnification fields. In this paper, the selected areas for FJC staining were roughly similar to the ischaemic peripheral areas shown here. (E) After EA or vehicle treatment, the number of damaged nerve cells in the 40× high-magnification fields is shown. Bars represent the mean \pm S.E.M. of 6 brains. *, $P < 0.05$ versus vehicle-treated ICH group.

of EA after ICH injury (Figure 4).

There are two steps involved in ICH damage, and the effect of haematoma in the early stage of ICH can lead to nerve tissue and cellular injury (19). The breakdown of blood cells contributes to the secondary damage after ICH; haemoglobin is known to be a toxic substance that leads to cell death via its effects on immune cells in pathological brain injury (20,21). Subsequently, iron degradation of haemoglobin induces lethal reactive oxygen species (ROS)

production and lipid peroxidation, which also contribute to secondary brain injury (22). In general, the pathological process that occurs after ICH involves complex molecular processes containing apoptosis cascades, inflammatory responses, brain oedema and ischaemia (23). Therefore, drug therapy for ICH faces complex pathological processes and plays a neuroprotective role during the interaction period of these pathological processes. Unfortunately, many drugs used for ICH treatment that have protective effects in

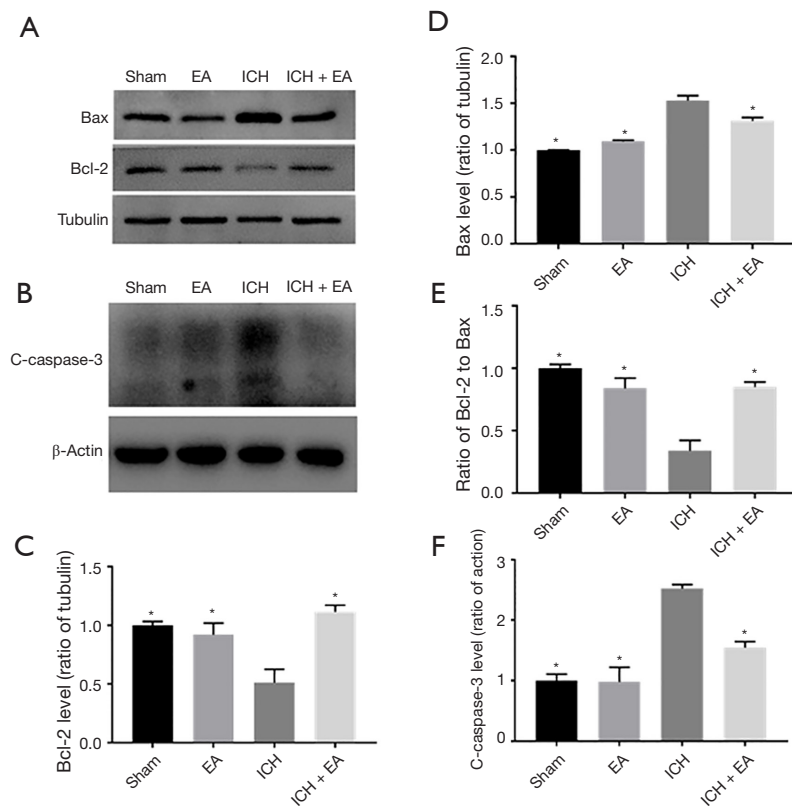


Figure 3 Echinocystic acid (EA) treatment reduced the expression of apoptosis-related proteins after intracerebral haemorrhage (ICH). Mice were treated with EA (50 mg/kg, i.p.) or vehicle once a day for 3 consecutive days after ICH. Western blot was used to detect the levels of apoptosis-related protein. (A) This picture shows the levels of Bcl-2, Bax and β -tubulin, with β -tubulin used as a loading control; (B) this picture shows the levels of cleaved caspase-3 and β -actin, with β -actin used as a loading control; (C) this picture shows the quantitative analysis of the ratio of Bcl-2 to β -tubulin; (D) this picture shows the quantitative analysis of the ratio of Bax to β -tubulin; (E) this picture shows the quantitative analysis of the ratio of Bcl-2 to Bax; (F) this picture shows the quantitative analysis of the ratio of cleaved caspase-3 to β -actin. EA treatment reduced the ratio of cleaved caspase-3 to β -actin and improved the ratio of Bcl-2 to Bax. The bar graph represents the mean \pm S.E.M. of 3 brains in each group, *, $P < 0.05$ compared with the ICH group.

animal experiments have failed in clinical trials. The toxicity of the agent itself may be one of the most important reasons for the appearance of this phenomenon (24).

Plant extracts, especially the plant components used in treatment with traditional Chinese medicine, are considered to represent an effective method for treating diseases because of the safety and special effects of these extracts in response to various pathological symptoms (25). EA, which is widely used in food production and Chinese medicine, has been reported to have antiviral, anti-tumour and anti-inflammatory effects (12,13,26). In recent years, EA has shown utility in different neurological diseases. Research has shown that EA can reduce the reserpine-induced pain/depression dyad in mice (27). Many studies have demonstrated that EA can improve

cognitive function and promote the growth of synapses (14). In our study, we tested the effect of EA on the third day after ICH establishment, and the time points assessed included different pathological stages after cerebral haemorrhage (28). EA treatment significantly improved the neurological function of mice after ICH (*Figure 1*). LFB staining showed that the volume of brain haematoma decreased significantly after EA intervention (*Figure 2D*). EA exhibited protective effects in the ICH mouse model. FJC staining has always been used to measure the level of neuron apoptosis (29). After initiating this experiment, we found that EA reduced neuron apoptosis after ICH injury compared with the control group (*Figure 2*). Therefore, we considered whether the neuroprotective effect of EA in ICH was closely related to

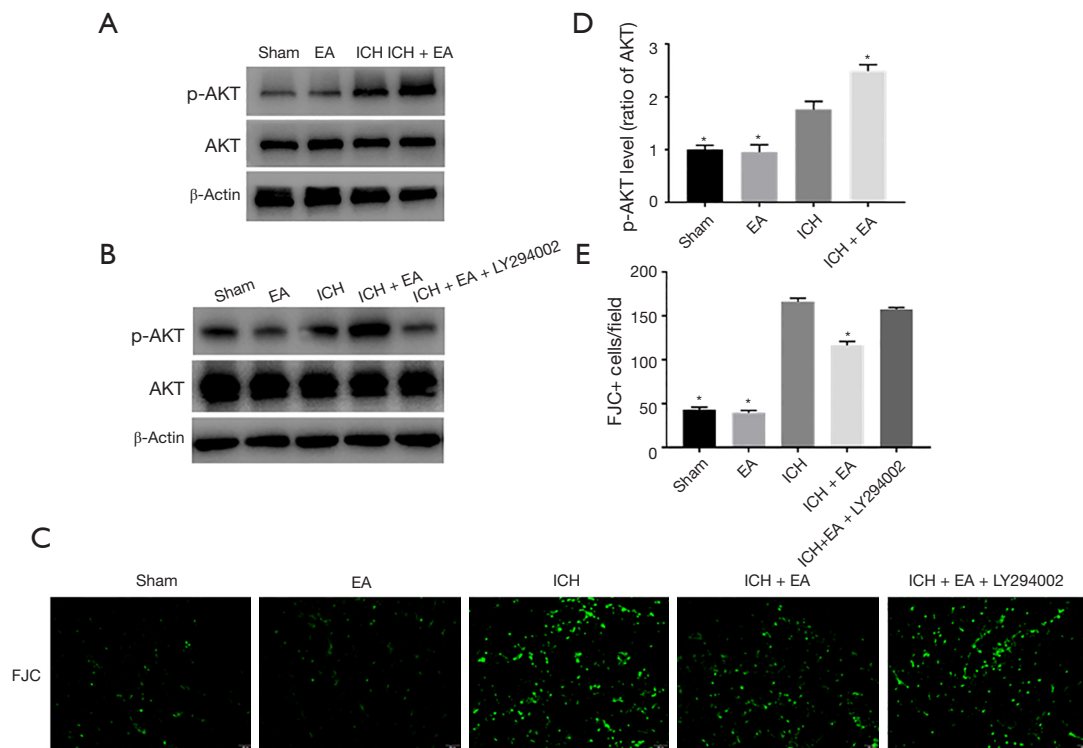


Figure 4 Echinocystic acid (EA) protected against cerebral intracerebral haemorrhage (ICH) injury by regulating the PI3K/AKT apoptosis signalling pathway. Mice were treated with EA (50 mg/kg, i.p.) or vehicle once a day for 3 consecutive days after ICH. In the ICH+EA+LY294002 group, mice were treated with the PI3K inhibitor LY294002 (i.p. 5 μ L of 10 mM LY-294002 dissolved in 3% DMSO) 15 min before cerebral haemorrhage once a day for 3 consecutive days. Cerebral tissue was collected, and protein levels were determined by Western blot. (A,B) The levels of p-AKT, AKT and β -actin. (C) Fluoro-jade C (FJC) staining images in each group. There were more positive cells in the ICH+EA+LY294002 group than in the ICH+EA group. (D) This picture shows the quantitative analysis of the ratio of p-AKT to AKT. The bar graph represents the mean \pm S.E.M. of 3 brains in each group, *, $P < 0.05$ compared with the ICH group. (E) The number of damaged nerve cells in the 40 \times high-magnification fields is shown. Bars represent the mean \pm S.E.M. of 6 brains. *, $P < 0.05$ versus vehicle-treated ICH group.

apoptosis.

Excessive apoptosis has been proven to be an important cause of nerve cell death in different pathological stages of ICH (30). Inhibiting apoptosis in nerve cells is considered to be the main target for alleviating the damage of nerve tissue and nerve function defects in cerebral haemorrhage (23). FJC staining reminded us of the potential anti-apoptotic characteristic of EA in ICH injury, although it has been reported that EA induces apoptosis in human liver cancer cells (15). However, Wu *et al.* found that EA resulted in an elevation of Bcl-2 mRNA levels in acute myocardial ischaemia rats (31). We used the specific indicators of apoptosis Bcl-2 and Bax. As expected, we found that EA treatment markedly increased the Bcl-2/Bax ratio after cerebral haemorrhage *in vivo*. To further confirm the anti-

apoptotic effect of EA, we measured the level of cleaved caspase-3, another classic apoptosis marker; EA was found to significantly downregulate the expression of cleaved caspase-3 after ICH. These results suggest that EA might play a vital role in modulating the progression of neuronal apoptosis in the ICH mouse model.

The protective mechanisms of EA in different diseases are still unclear. Joh *et al.* found that EA ameliorated lung inflammation by inhibiting the binding of LPS to TLR4 in the NF- κ B and MAPK pathways in mice (12). Hyam *et al.* also demonstrated that EA inhibited TNBS-induced colitis in mice by blocked the binding of LPS to TLR4 (13). Similarly, EA has also been reported to have anti-inflammatory effects via its inhibition of IL-1 β induced NF- κ B and mitogen-activated protein kinase (MAPK)

activation in human osteoarthritic chondrocytes (32). Although some studies have shown that EA is an underlying factor in hypolipidaemic activity as assessed by cholesterol acyltransferase and diacylglycerol acyltransferase, the relevant signalling pathway that serves as a mechanism in this process is still unclear (33). Increasing evidence has demonstrated that intracellular signalling pathways are changed by EA treatment. In HL-60 cells, EA induced apoptosis through an ROS-independent mitochondrial dysfunction pathway (34). In HepG2 cells, EA activated the JNK pathway and P38 kinase, leading to apoptosis in HepG2 cells (15). Few studies have confirmed the mechanism of EA in the nervous system. Park *et al.* demonstrated that EA treatment promoted neurite outgrowth in neuroblastoma neuro2a cells through the JNK signalling pathway in aged mice (14). In the vascular system, EA protected endothelial progenitor cells from damage caused by oxLDL via the AKT/eNOS pathway (35). Since our data demonstrated protective effects of EA, we further examined the effect of EA on signalling pathways after ICH injury. Numerous studies have shown that the PI3K/AKT pathway is an important protective signalling pathway in stroke damage, and the activation of the PI3K/AKT pathway has also been shown to have anti-apoptotic effects *in vivo* and *in vitro* (36). There has been no evidence that shows whether EA activates the PI3K/AKT pathway after ICH injury. In our study, we explored whether EA treatment improved the level of p-AKT, which demonstrates the activation of the PI3K/AKT pathway. The neuroprotective effects of EA were abolished by LY294002 (an inhibitor of the PI3K/AKT pathway) after ICH injury (Figure 4). According to FJC staining, the neuronal apoptosis level was reduced by EA treatment; however, LY294002 reversed these effects.

In summary, our study shows that EA provides neuroprotective effects after ICH injury on haematoma volume and neuronal apoptosis. EA exhibits the pharmacologic action of activation of the PI3K/AKT pathway to achieve its anti-apoptotic effects. As a plant extract and an ingredient in traditional Chinese medicine, EA has high potential for use as a drug in clinical trials for ICH treatment.

Acknowledgments

Funding: This research was funded by the National Natural Science Foundation of China (81400963), Jiangsu Province Key Medical Discipline (ZDXKA2016020), and Jiangsu Provincial Medical Youth Talent (Grant #QNRC2016327

and #QNRC2016328). Yangzhou 13th Five-Year Science and Education Key Talent Fund (ZDRC54, ZDRC55).

Footnote

Conflicts of Interest: The authors have no conflicts of interest to declare.

Ethical Statement: The authors are accountable for all aspects of the work in ensuring that questions related to the accuracy or integrity of any part of the work are appropriately investigated and resolved. All experimental procedures were approved by the Animal Ethics Committee of Yangzhou University (license number: YIACUC-14-0014).

References

1. Qureshi AI, Mendelow AD, Hanley DF. Intracerebral haemorrhage. *Lancet* 2009;373:1632-44.
2. Mracsko E, Veltkamp R. Neuroinflammation after intracerebral hemorrhage. *Front Cell Neurosci* 2014;8:388.
3. Xi G, Strahle J, Hua Y, et al. Progress in translational research on intracerebral hemorrhage: is there an end in sight? *Prog Neurobiol* 2014;115:45-63.
4. Zhao X, Sun G, Zhang J, et al. Hematoma resolution as a target for intracerebral hemorrhage treatment: role for peroxisome proliferator-activated receptor gamma in microglia/macrophages. *Ann Neurol* 2007;61:352-62.
5. Wu H, Wu T, Xu X, et al. Iron toxicity in mice with collagenase-induced intracerebral hemorrhage. *J Cereb Blood Flow Metab* 2011;31:1243-50.
6. Wang J. Preclinical and clinical research on inflammation after intracerebral hemorrhage. *Prog Neurobiol* 2010;92:463-77.
7. Righy C, Bozza MT, Oliveira MF, et al. Molecular, Cellular and Clinical Aspects of Intracerebral Hemorrhage: Are the Enemies Within? *Curr Neuropharmacol* 2016;14:392-402.
8. Zhao X, Wu T, Chang CF, et al. Toxic role of prostaglandin E2 receptor EP1 after intracerebral hemorrhage in mice. *Brain Behav Immun* 2015;46:293-310.
9. Liao XY, Lei Y, Chen SF, et al. The neuroprotective effect of bisperoxovandium (pyridin-2-squaramide) in intracerebral hemorrhage. *Drug Des Devel Ther* 2019;13:1957-67.
10. Lai P, Du JR, Zhang MX, et al. Aqueous extract of *Gleditsia sinensis* Lam. fruits improves serum and liver lipid profiles and attenuates atherosclerosis in rabbits fed a high-fat diet. *J Ethnopharmacol* 2011;137:1061-6.
11. Lee KT, Choi J, Jung WT, et al. Structure of a new echinocystic acid bisdesmoside isolated from

- Codonopsis lanceolata roots and the cytotoxic activity of prosapogenins. *J Agric Food Chem* 2002;50:4190-3.
12. Joh EH, Gu W, Kim DH. Echinocystic acid ameliorates lung inflammation in mice and alveolar macrophages by inhibiting the binding of LPS to TLR4 in NF-kappaB and MAPK pathways. *Biochem Pharmacol* 2012;84:331-40.
 13. Hyam SR, Jang SE, Jeong JJ, et al. Echinocystic acid, a metabolite of lancemaside A, inhibits TNBS-induced colitis in mice. *Int Immunopharmacol* 2013;15:433-41.
 14. Park HJ, Kwon H, Lee S, et al. Echinocystic Acid Facilitates Neurite Outgrowth in Neuroblastoma Neuro2a Cells and Enhances Spatial Memory in Aged Mice. *Biol Pharm Bull* 2017;40:1724-9.
 15. Tong X, Lin S, Fujii M, et al. Molecular mechanisms of echinocystic acid-induced apoptosis in HepG2 cells. *Biochem Biophys Res Commun* 2004;321:539-46.
 16. Huang CF, Wang WN, Sun CC, et al. Echinocystic acid ameliorates hyperhomocysteinemia-induced vascular endothelial cell injury through regulating NF-kappaB and CYP1A1. *Exp Ther Med* 2017;14:4174-80.
 17. Yu H, Li W, Cao X, et al. Echinocystic acid, a natural plant extract, alleviates cerebral ischemia/reperfusion injury via inhibiting the JNK signaling pathway. *Eur J Pharmacol* 2019;861:172610.
 18. Bonsack F, Sukumari-Ramesh S. Differential Cellular Expression of Galectin-1 and Galectin-3 After Intracerebral Hemorrhage. *Front Cell Neurosci* 2019;13:157.
 19. Xi G, Keep RF, Hoff JT. Erythrocytes and delayed brain edema formation following intracerebral hemorrhage in rats. *J Neurosurg* 1998;89:991-6.
 20. Akyol GY, Manaenko A, Akyol O, et al. IVIG activates FcgammaRIIB-SHIP1-PIP3 Pathway to stabilize mast cells and suppress inflammation after ICH in mice. *Sci Rep* 2017;7:15583.
 21. Schaer CA, Schoedon G, Imhof A, et al. Constitutive endocytosis of CD163 mediates hemoglobin-heme uptake and determines the noninflammatory and protective transcriptional response of macrophages to hemoglobin. *Circ Res* 2006;99:943-50.
 22. Wan J, Ren H, Wang J. Iron toxicity, lipid peroxidation and ferroptosis after intracerebral haemorrhage. *Stroke Vasc Neurol* 2019;4:93-5.
 23. Qureshi AI, Suri MF, Ostrow PT, et al. Apoptosis as a form of cell death in intracerebral hemorrhage. *Neurosurgery* 2003;52:1041-7; discussion 1047-8.
 24. Han L, Ni Y, Cao M, et al. A New Role Discovered for IGTP: The Protective Effect of IGTP in ICH-Induced Neuronal Apoptosis. *Cell Mol Neurobiol* 2016;36:713-24.
 25. Li P, Tang T, Liu T, et al. Systematic analysis of tRNA-derived small RNAs reveals novel potential therapeutic targets of traditional chinese medicine (buyang-huanwu-decoction) on intracerebral hemorrhage. *Int J Biol Sci* 2019;15:895-908.
 26. Wang H, Yu F, Peng Y, et al. Synthesis and biological evaluation of ring A and/or C expansion and opening echinocystic acid derivatives for anti-HCV entry inhibitors. *Eur J Med Chem* 2015;102:594-9.
 27. Li S, Han J, Wang DS, et al. Echinocystic acid reduces reserpine-induced pain/depression dyad in mice. *Metab Brain Dis* 2016;31:455-63.
 28. Cheng Y, Wei Y, Yang W, et al. Cordycepin confers neuroprotection in mice models of intracerebral hemorrhage via suppressing NLRP3 inflammasome activation. *Metab Brain Dis* 2017;32:1133-45.
 29. Li Q, Wan J, Lan X, et al. Neuroprotection of brain-permeable iron chelator VK-28 against intracerebral hemorrhage in mice. *J Cereb Blood Flow Metab* 2017;37:3110-23.
 30. Ni H, Shen J, Song Y, et al. EP3, Prostaglandin E2 receptor subtype 3, associated with neuronal apoptosis following intracerebral hemorrhage. *Cell Mol Neurobiol* 2016;36:971-80.
 31. Wu J, Li J, Zhu Z, et al. Protective effects of echinocystic acid isolated from *Gleditsia sinensis* Lam. against acute myocardial ischemia. *Fitoterapia* 2010;81:8-10.
 32. Ma Z, Wang Y, Piao T, et al. Echinocystic Acid Inhibits IL-1beta-Induced COX-2 and iNOS expression in human osteoarthritis chondrocytes. *Inflammation* 2016;39:543-9.
 33. Han L, Lai P, Du JR. Deciphering molecular mechanism underlying hypolipidemic activity of echinocystic Acid. *Evid Based Complement Alternat Med* 2014;2014:823154.
 34. Tong X, Lin S, Fujii M, et al. Echinocystic acid induces apoptosis in HL-60 cells through mitochondria-mediated death pathway. *Cancer Lett* 2004;212:21-32.
 35. Lai P, Liu Y. Echinocystic acid, isolated from *Gleditsia sinensis* fruit, protects endothelial progenitor cells from damage caused by oxLDL via the Akt/eNOS pathway. *Life Sci* 2014;114:62-9.
 36. Yu H, Zhang ZL, Chen J, et al. Carvacrol, a food-additive, provides neuroprotection on focal cerebral ischemia/reperfusion injury in mice. *PLoS One* 2012;7:e33584.

Cite this article as: Chen B, Zhao Y, Li W, Hang J, Yin M, Yu H. Echinocystic acid provides a neuroprotective effect via the PI3K/AKT pathway in intracerebral haemorrhage mice. *Ann Transl Med* 2020;8(1):6. doi: 10.21037/atm.2019.12.35